5. Chapter 5. Tailoring of the deposition process to obtain reliable SBT capacitors for high density FRAMs

5.1 Abstract

Crystallization of $SrBi_2Ta_2O_9$ (SBT) thin films was studied as a function of viscosity of bismuth precursor and baking temperature, in order to fabricate capacitors with improved ferroelectric properties. SBT thin films were deposited on to Pt substrates using a chemical solution deposition (CSD) technique. Post-deposition anneal at 750 ^{0}C for 1 hour in oxygen atmosphere revealed a significant influence of baking temperature and the viscosity of bismuth precursor on the microstructure and the ferroelectric properties of SBT thin films. A higher baking temperature (350 ^{o}C) and a lower viscosity of bismuth precursor (8 cp) yielded larger amounts of Bi_2O_3 secondary phase, smaller SBT grains (104 nm) and lower remanent polarization (P_r = 2.0 □c/cm^2). Additionally, these films exhibited a very high rate of ageing (>45 % reduction in Pr after 7 days). A modified CSD process is suggested, which could suppress the formation of Bi_2O_3 secondary phase. Films fabricated using modified CSD technique exhibited a much larger grain size of 165 nm, higher P_r of 7.2 □c/cm^2, and significantly improved ageing characteristics (< 1% reduction in P_r after 7 days). A qualitative model to describe the ageing in SBT based capacitors is also suggested.

5.2 Introduction

Chemical solution deposition process (CSD) is one of the commonly used techniques to deposit fatigue-free $SrBi_2Ta_2O_9$ (SBT) thin films [1]. In literature, several processing parameters such as the annealing temperature and annealing method, annealing gas, stoichiometry and the chemical formula of the precursors were studied extensively and were reported to affect the ferroelectric properties [2-12]. However, there is a wide variation in the reported remanent polarization (P_r ranging from 4μC/cm^2 to 10 μC/cm^2) of SBT thin film capacitors deposited under almost identically maintained above mentioned processing conditions.

Even within our own group, earlier, we reported a P_r of 6.5 □C/cm^2 for SBT thin film capacitors fabricated using a room temperature stable precursor solution [2]. However, we have significant variations in these results when a different batch of Bi precursor, belonging to the same vendor was used. Additionally, SBT thin film capacitors fabricated using Bi precursors bought from different vendors, exhibited widely varying ferroelectric properties (Figure 5.1). The only difference was in the viscosity of the Bi precursor. Therefore, the viscosity of the Bi precursor is an important processing parameter that could affect the ferroelectric properties of SBT thin films.

Viscosity may be indicative of the molecular nature, more importantly extent of oligemerization of Bi precursor. The extent of oligemerization of Bi precursor could influence the crystallization of Bi_2O_3. Pure Bi precursors, when coated on Pt substrates and baked, revealed a dependence of crystallization of Bi_2O_3 on the viscosity of the precursor (Figure 5.2). Since, the crystallization temperature of Bi_2O_3 is close to the typical baking temperatures of SBT thin

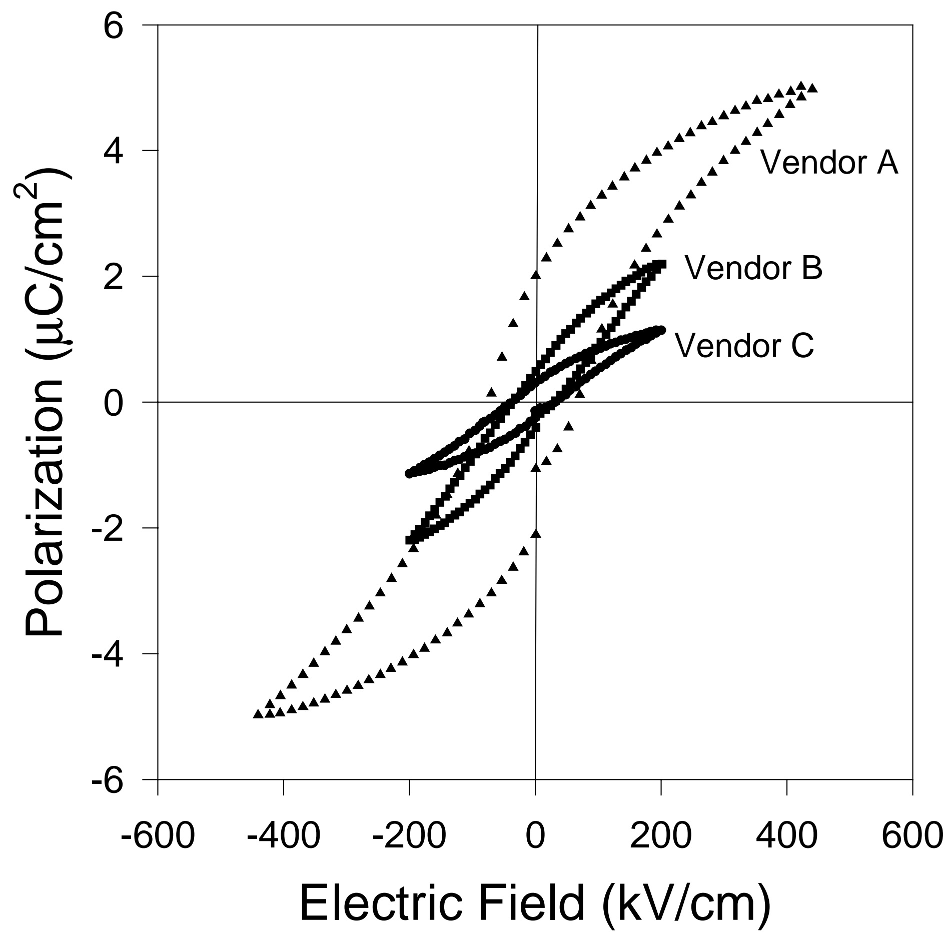

Fig 5.1 Variation of hysteresis loops exhibited by SBT thin film capacitors fabricated using bismuth precursor obtained from different vendors.

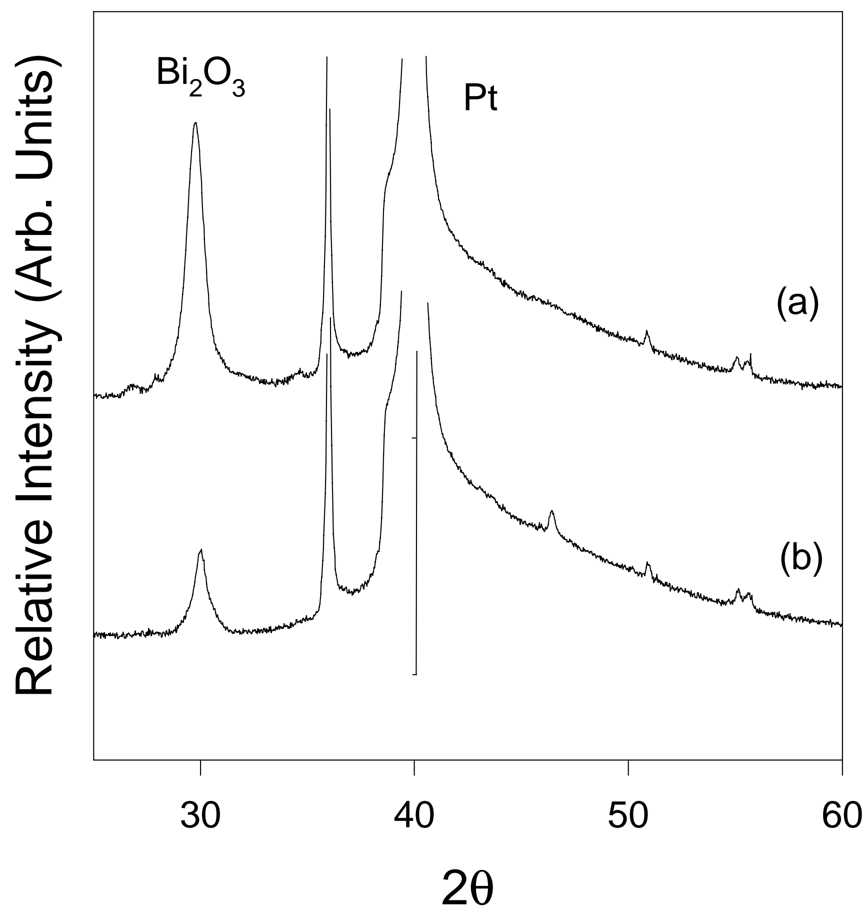

Fig 5.2 XRD patterns of Bi2O3 thin films on Pt substrates obtained by coating pure bismuth precursor possessing a viscosity of (a) 8 cp; (b) 15 cp; and followed by baking at 500 0C.

films (~ 450 ^{0}C), a secondary phase of Bi_2O_3 could be formed in the SBT thin films during baking. Hence, viscosity of Bi precursor and baking temperature could influence the formation of Bi_2O_3 secondary phase in SBT thin films prior to high temperature anneal. Presence of the Bi_2O_3 secondary phase could effect the crystallization kinetics of the SBT thin films during high temperature annealing.

There have been reports of the presence of Bi_2O_3 secondary phase in crystallized SBT thin films[13]. However, no correlation was established between the amount of the Bi_2O_3 secondary phase and the ferroelectric properties of the capacitors. In this study, we investigated the dependence of the amount of the Bi_2O_3 secondary phase on the viscosity and the baking temperature. The sensitivity of the ferroelectric properties of SBT thin films on the amount of secondary Bi_2O_3 phase was studied. A modified CSD technique was developed to minimize this secondary phase in the crystallized SBT thin films, and thereby obtain improved ferroelectric properties. Additionally we also examined the ageing characteristics of SBT thin films as a function of the amount of the Bi_2O_3 secondary phase. A qualitative model to explain ageing in SBT thin films is proposed.

5.3 Experimental

SBT thin films were fabricated by chemical solution deposition technique, as shown in Fig. 5.3. The precursors for Sr and Ta used were Sr-acetate (Alfa Aesar) and Ta-ethoxide (Inorgatech) respectively. In case of Bi precursor, we prepared bismuth 2-ethyl hexanoate by dissolving Bi_2O_3 in 2-ethyl hexanoic acid at 180 ^{0}C followed by stirring at the same temperature for a varying length of time. Increasing the stirring time increased the viscosity of Bi precursor. Initially, clear solutions of Sr-acetate in acetic acid and Ta-ethoxide in 2-methoxy ethanol were prepared. After bringing the bismuth precursor to the room temperature, all the three precursors

were mixed to form a homogeneous 0.1 M solution with 15% excess bismuth amount. This solution was used to spin coat the $Pt/TiO_2/Si$ substrates at 6000 rpm for one minute. After each coating films are baked on a hot plate. The hot plate temperature (also known as baking temperature) is varied from 150 ^{0}C to 350 ^{0}C. This procedure of coating the films and baking was repeated until a total thickness of the film of 0.25 μm is achieved. For the present study, four different SBT thin films are prepared by using two different viscosities of Bi-2-ethyl hexanoate and two different baking temperatures. For convenience, we will represent these samples by mentioning the viscosity of the Bi-2-ethyl hexanoate and the baking temperature in the notation 'X cp/ Y ^{0}C'. For instance, '15 cp/ 150 ^{0}C SBT thin film' would mean that SBT samples are coated using a solution in which the viscosity of Bi-2-ethyl hexanoate is 15 cp and the as-coated samples are baked at a temperature of 150 ^{0}C. A final anneal at a high temperature of 750 ^{0}C was given to all the films for 1.5 hours in a conventional tube furnace in oxygen atmosphere.

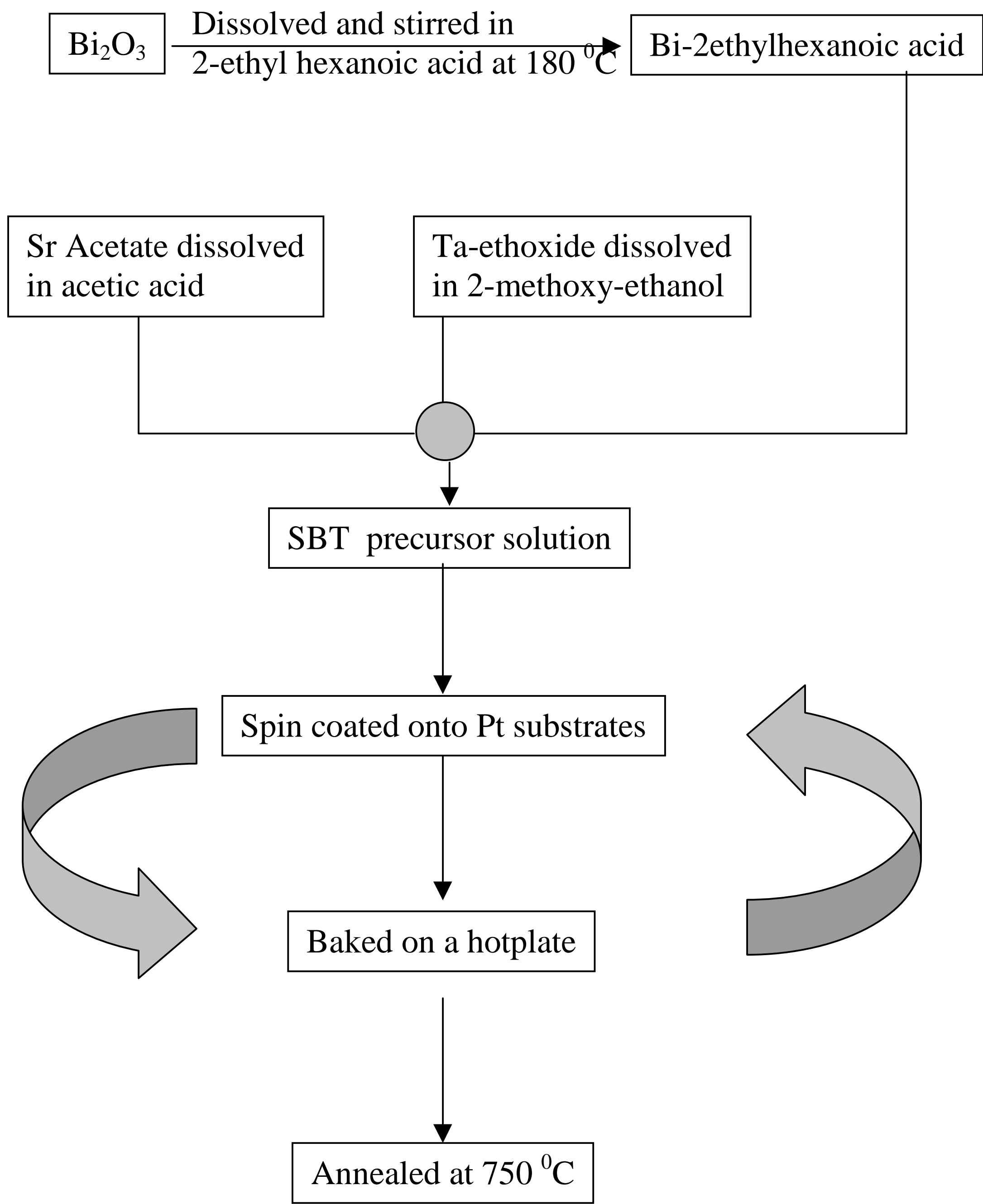

Fig. 5.3. Conventional method for preparation of SBT thin films.

An array of circular Pt electrodes with a nominal area of 3 x 10^{-4} cm^2 was sputter deposited on to the top surface of SBT thin film using a shadow mask for measuring electrical properties. Ferroelectric properties of these thin film capacitors were measured using the RT66A ferroelectric tester made by Radiant Technologies. X-ray diffraction was performed using the Scintag DMS 2000 x-ray diffractometer, with the Cu K_α radiation (λ = 1.54056) at a scanning speed of 2 ^{0}/minute. Microstructure of the annealed thin films was determined using field-emission scanning electron microscope (FESEM Hitachi S-4500S, 5 kV).

5.4. Results and Discussion

5.4.1 As-baked SBT thin films

Fig. 5.4 shows the x-ray diffraction pattern of the as-baked SBT thin films. We could observe a broad peak around 30°, which corresponds to the presence of fine grained Bi_2O_3 second phase in SBT thin films. From Fig. 5.4(a) and 5.4(b), we could observe that the FWHM and the total intensity of the broad peak of the baked films follows the order: 8 cp/350 ^0C > 8 cp/150 ^0C > 15 cp/350 ^0C > 15 cp/150 ^0C. This indicates that lower viscosity of Bi precursor and higher baking temperature yields larger amounts of Bi_2O_3 second phase. Consequently, minimal formation of Bi_2O_3 secondary phase is obtained in the films prepared by using higher viscosity of Bi-precursor and lower baking temperature, namely, 15 cp/150 ^0C SBT samples. Hence, formation of Bi_2O_3 secondary phase in SBT thin films was initiated during baking of the films and its amount is strongly dependent on the viscosity of the bismuth precursor as well as the baking temperature. Formation of Bi_2O_3 in SBT films prior to the high temperature anneal could affect the crystallization of SBT during high temperature annealing.

5.4.2 SBT thin films after high temperature Anneal

Fig. 5.5 shows XRD of SBT thin films after annealing at 750 ^0C, as a function of viscosity of bismuth precursor as well as the baking temperature. All the films were found to crystallize with no c-axis orientation. However, a significant influence of viscosity of the bismuth precursor and the baking temperature was found on the amounts of Bi_2O_3 secondary phase formed in the crystallized SBT thin films. We found that the ratio of relative intensity of Bi_2O_3 peak to that of (115) peak of SBT, which is

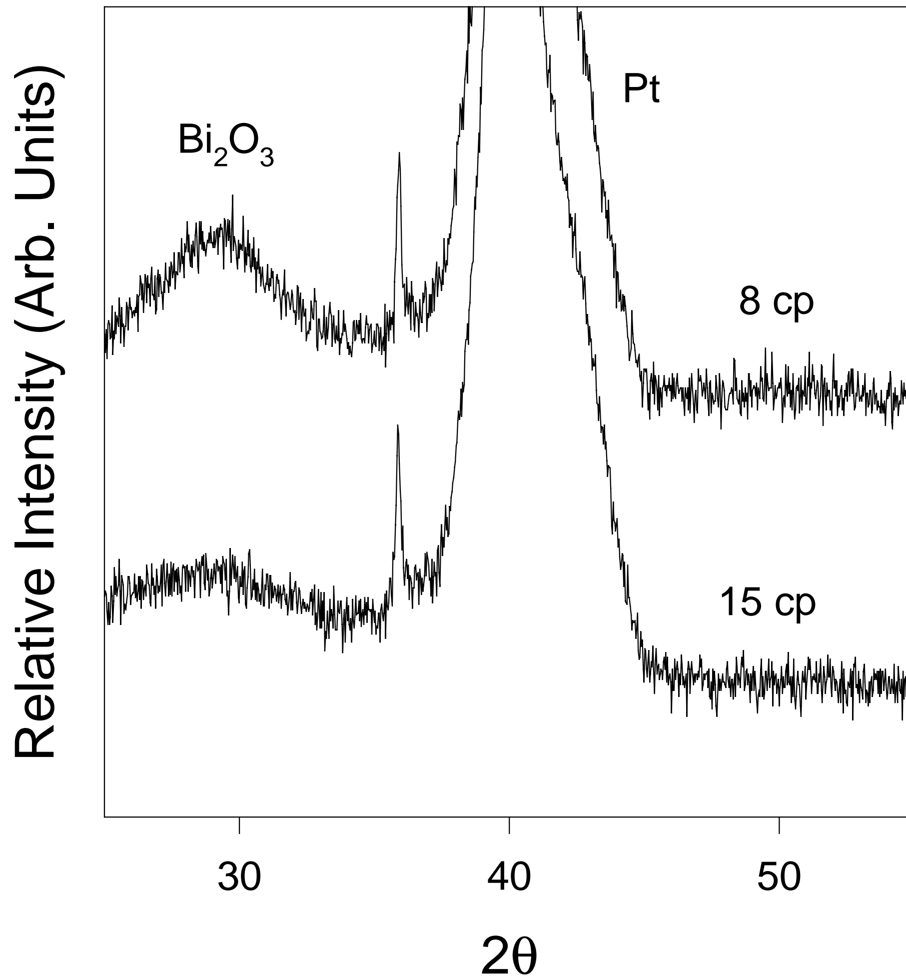

Fig 5.4a XRD patterns of as-baked SBT thin films deposited using various viscosities of bismuth precursor followed by baking at 350 ^{0}C.

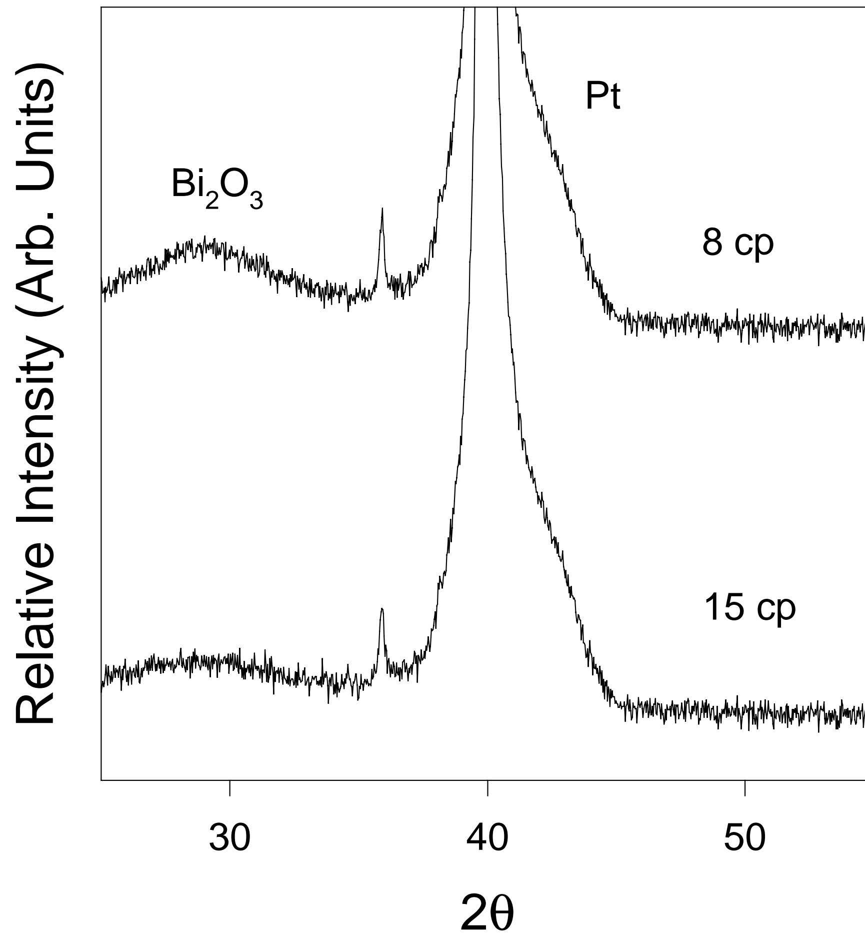

Fig 5.4b XRD patterns of as-baked SBT thin films deposited using various viscosities of bismuth precursor followed by baking at 150 ^{0}C.

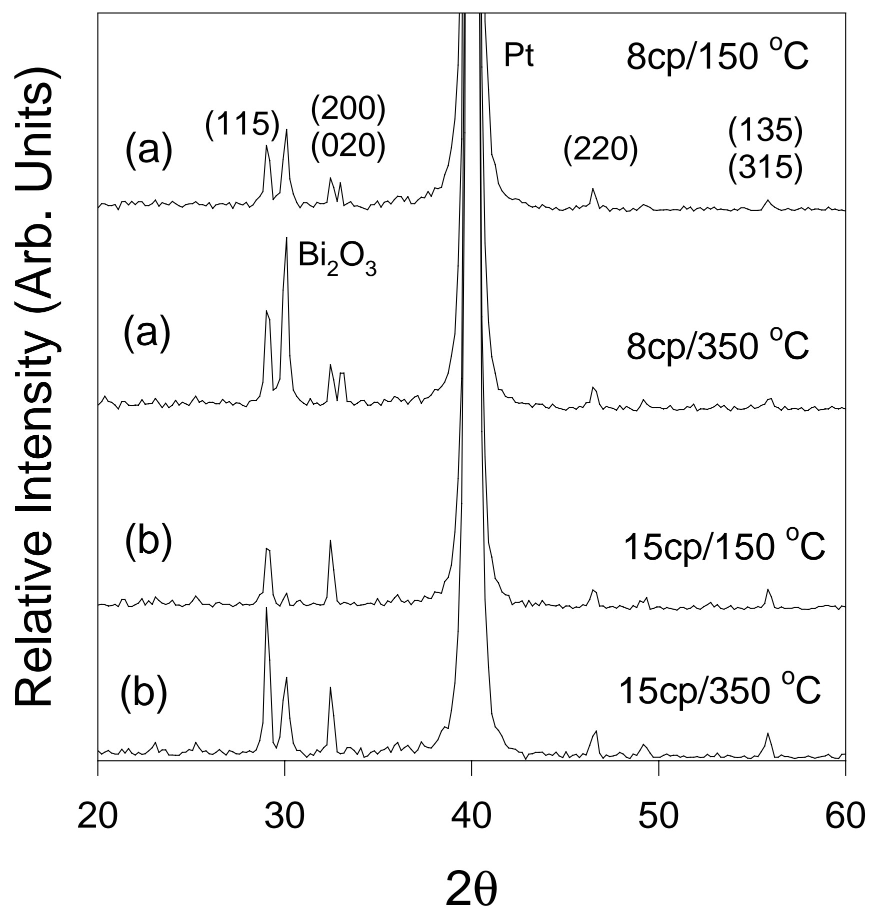

Fig 5.5 XRD patterns of crystallized SBT thin films deposited on Pt substrates using various viscosities of bismuth precursor and baking temperatures followed by annealing at 750 ^{0}C.

proportional to the relative amounts of Bi_2O_3 secondary phase, is in the order 8 cp/350 ^{0}C > 8 cp/150 ^{0}C > 15 cp/350 ^{0}C > 15 cp/150 ^{0}C .

(From here on we will refer to this ratio as "*f*"). Lower viscosity of Bi precursor and higher baking temperature resulted in larger amounts of Bi_2O_3 second phase after annealing, which is similar to that observed in as-baked SBT thin films. This can be explained as follows.

In a CSD process, before the thin film is subjected to high temperature anneal, the SBT thin film would predominantly contain a network of Sr, Bi, Ta and O atoms in an amorphous form. A high temperature anneal is necessary to obtain bismuth layered phase of SBT. Crystallization of SBT could occur in two routes: (I) Direct crystallization of bismuth layered phase of SBT from the amorphous phase; (II) Formation of individual elements or oxides of one or more elements and their subsequent reaction to form bismuth layered phase. Crystallization of SBT through path (II) would require a very high temperature of annealing (>>750 ^{0}C) and thereby, annealing at 750 ^{0}C could result in some unreacted oxides.

Presence of Bi_2O_3 secondary phase in our SBT thin films prior to the high temperature anneal, as seen in Fig. 5.4, could lead to a combination of both the crystallization paths. Consequently we observed the presence of unreacted Bi_2O_3 seen as a secondary phase (Fig. 5.5) after high temperature anneal. Further evidence of the presence of Bi_2O_3 as a secondary phase was obtained from the microstructure analysis.

Fig. 5.6 shows the FESEM micrographs of surfaces of crystallized SBT thin films deposited using different viscosities of bismuth precursor and baking temperature. All the

films show rod-like SBT grains with no observable platelet structures. This indicates the absence of c-axis orientation which is also observed in the XRD patterns of these films (Fig. 5.5). Along with the rod-like SBT grains, bright circular spots with an average size of 35 nm could be found in the micrographs of almost all the sample surfaces. These bright spots were confirmed as bismuth oxide in the x-ray microanalysis mode of FESEM. Large amounts of Bi_2O_3 secondary phase seen in the XRD pattern of 8 cp/350 ^{0}C sample (Fig. 5.5a) is reflected as large number of bright spots seen in the micrograph of the same sample (Fig. 5.6a). Additionally, amount of these secondary phases present in the SBT films follow the order : 8 cp/ 350 ^{0}C > 8 cp/ 150 ^{0}C > 15 cp/ 350 ^{0}C > 15 cp/ 150 ^{0}C, which is similar to the order obtained by calculating relative amounts of the secondary phases using XRD patterns (Fig. 5.5). Average SBT grain sizes of these thin films are tabulated in Table 5.1 as a function of *f* and processing conditions. We observed a significant effect of viscosity of the bismuth precursor and the baking temperature on the grain size of the SBT thin films. From Table 5.1, it is clear that higher viscosity and lower baking temperatures yields larger SBT grains. Such a trend could be explained by observing that the same processing conditions also resulted in smaller amounts of Bi_2O_3 secondary phase. Formation of Bi_2O_3 secondary phase could affect the SBT grain growth. Bi present in the SBT phase helps in grain growth as the mobility of Bi is very high as compared to that of other elements in SBT. Whereas Bi_2O_3 present as secondary phase would reduce the amount of Bi in the SBT phase and hence would hinder the grain growth [14]. In addition to the presence of Bi_2O_3 secondary phase, we also observed a bimodular distribution of grain sizes. While the large grains (grain size > 100nm) had a stoichiometry close to that of SBT, the smaller grains (grain size ranging from 45 nm-55

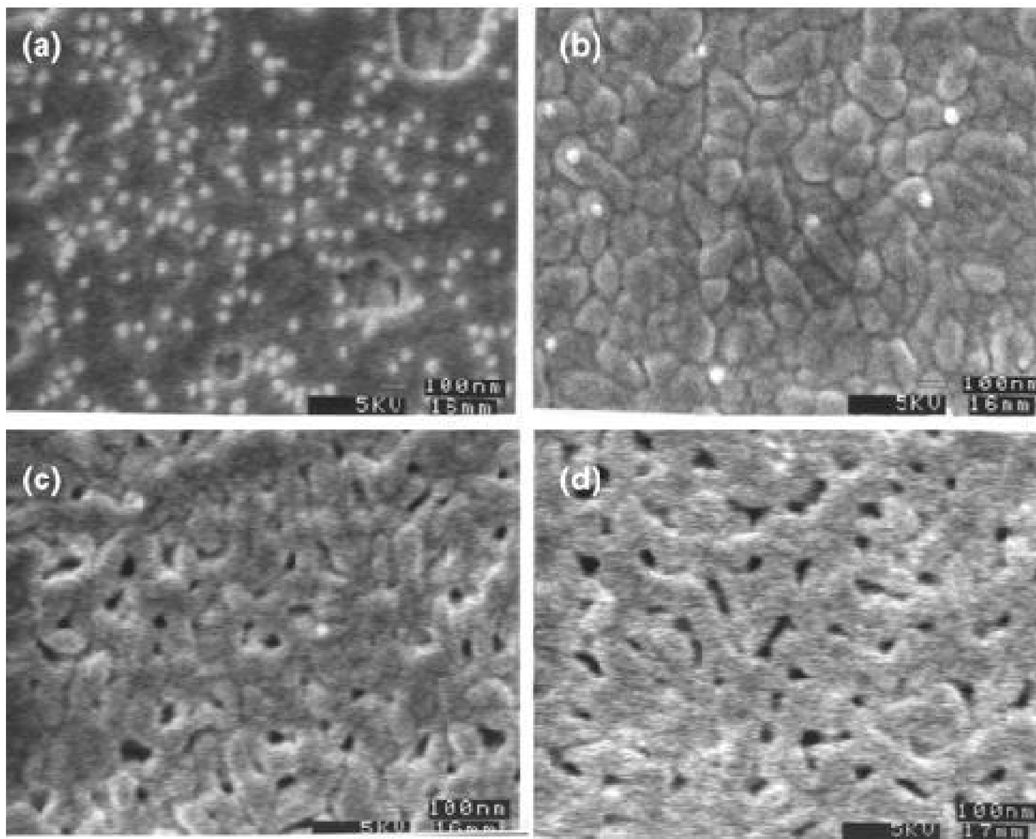

Fig. 5.6 FESEM micrographs of surfaces of crystallized SBT thin films deposited using conditions (a) 8cp/350 ^{0}C, (b) 8cp/150 ^{0}C, (c) 15cp/350 ^{0}C and (d) 15cp/350 ^{0}C

Table 5.1 Relative amounts of Bi_2O_3 secondary phase (f), grain size, remanent polarization (P_r), coercive fields (E_c & $-E_c$) as a function of stirring time of bismuth precursor and the baking temperature of crystallized SBT thin films.

Sample	**f**	**Grain size (nm)**	**P_r ($\mu C/cm^2$)**	**E_c (kV/cm)**	**$-E_c$ (kV/cm)**	**ΔE_c (kV/cm)**
8 cp/350 ^{0}C	1.4	104	2.0	34	-20	14
8 cp/150 ^{0}C	1	122	2.5	34	-25	9
15 cp/350 ^{0}C	0.4	130	4.0	42	-33	7
15 cp/150 ^{0}C	0.2	145	6.3	38	-34	4

nm) possessed a large bismuth deficiency. Such a trend was also observed by Koiwa et al who had shown that these smaller grains, consisting of fluorite type crystal structure, are paraelectric in nature[13]. Formation of large amounts of Bi_2O_3 secondary phase in a SBT film could result in SBT grains with bismuth deficiency, as was observed in our study. Thus, formation of Bi_2O_3 secondary phase, which depended on the viscosity of the bismuth precursor and the baking temperature, was found to have a significant impact on the microstructure of SBT thin films. It was observed that among all the films studied, 15 cp/150 ^{0}C possessed the largest grain size with the least amount of Bi_2O_3 secondary phase and minimal bimodular distribution. Homogenous composition of SBT grains with minimal secondary phase in these films could have been due to predominant direct crystallization of SBT from amorphous phase.

Based on the above analyses, it can be suggested that direct crystallization can be made feasible by carefully maintaining the baking temperature always lower than the Bi_2O_3 formation temperature. However, care should be taken to bake the thin film after each coating long enough to evaporate all the solvents from the thin film. Also, no intermediate temperature between the baking temperature and the annealing temperature should be seen by the SBT sample in order to minimize the formation of Bi_2O_3. These conditions would aid in obtaining near-stoichiometric SBT thin films with uniform microstructure and minimal Bi_2O_3 secondary phase formation.

Since the microstructure and composition of SBT thin films are two important factors that govern the ferroelectric properties [14], we have systematically studied the effects of processing conditions on the hysteresis properties of SBT capacitors.

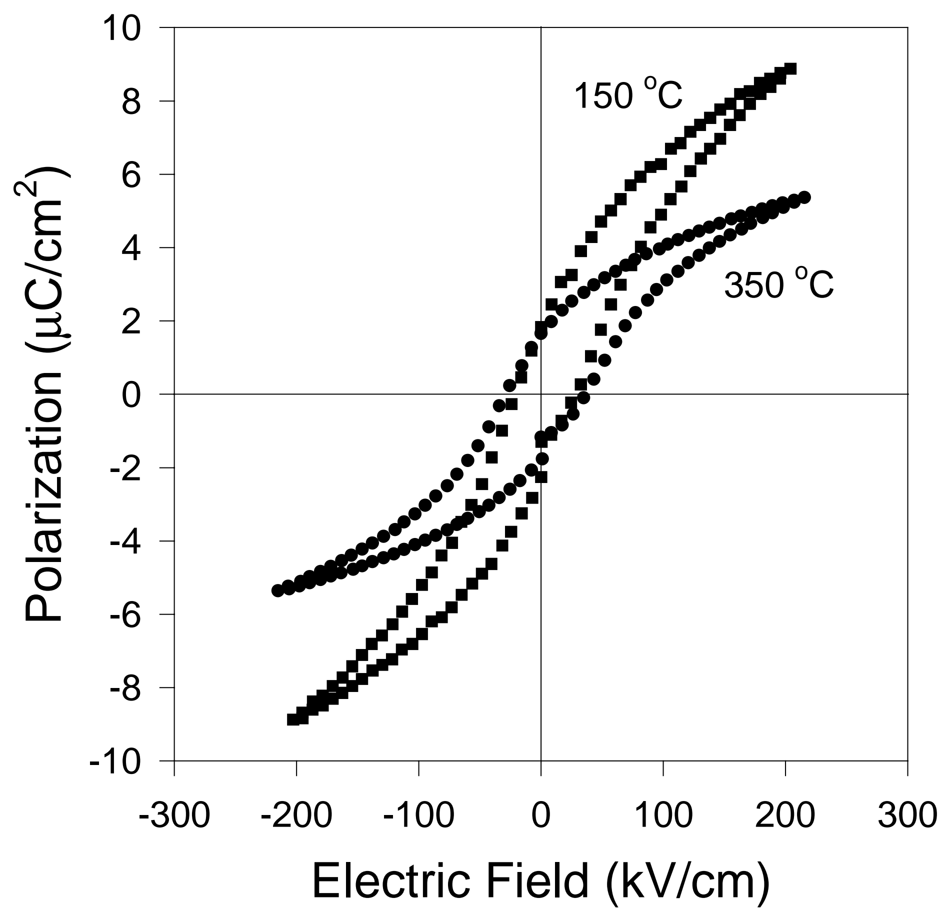

Fig. 5.7 Hysteresis loops of SBT thin film capacitor fabricated using a bismuth precursor with a viscosity of (a) 8 cp and (b) 15 cp; baking temperatures of 150 ^{0}C or 350 ^{0}C; and an annealing temperature of 750 ^{0}C.

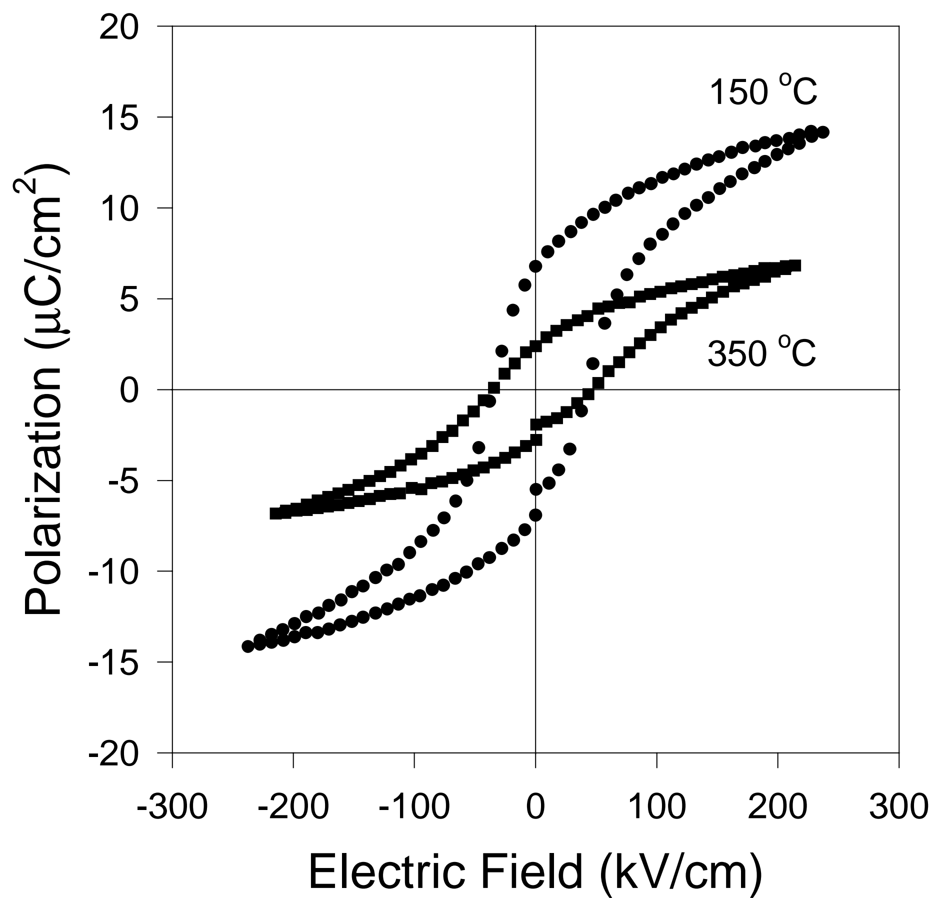

Fig. 5.7 Hysteresis loops of SBT thin film capacitor fabricated using a bismuth precursor with a viscosity of (a) 8 cp and (b) 15 cp; baking temperatures of 150 ^{0}C or 350 ^{0}C; and an annealing temperature of 750 ^{0}C.

5.4.3 Ferroelectric Properties of SBT capacitors

Fig. 5.7a and 5.7b, show the P-E hysteresis loops of SBT thin films prepared by varying the viscosity of bismuth precursor and the baking temperature. While all the capacitors exhibited well saturated hysteresis loops, they differed in the magnitudes of remanent polarization (P_r) and the coercive field (E_c). The average values of P_r and E_c are shown in Table I. While a lower P_r (2.0 $\mu C/cm^2$) was obtained in the 8 cp/350 ^0C SBT capacitors, 15 cp/150 ^0C capacitors showed a higher P_r of 6.3 $\mu C/cm^2$. In general, capacitors fabricated using higher viscosity of bismuth precursor and lower baking temperature exhibited a higher P_r while the average coercive fields of all the samples were found to be around 38 kV/cm. This trend could be explained by observing the strong correlation between the amount of the Bi_2O_3 (which is a function of processing parameters) and the remanent polarization (Table I). Orientation, grain size and stoichiometry are three important factors that govern P_r in SBT thin film capacitors [11-14]. Fig. 5.5 shows that there is no noticeable change in the orientation of the SBT thin films fabricated under different processing parameters. Therefore, the variation in P_r could be explained by the dependence of grain size and composition of SBT on the amount of the Bi_2O_3 secondary phase in these films. As discussed previously, smaller amounts of Bi_2O_3 secondary phase have yielded larger grain size and lesser deficiency of Bi in SBT grains. Larger grain size and lesser deficiency of Bi in a crystallized SBT thin film generally yields a higher remanent polarization [14]. Accordingly, SBT thin films with larger grain sizes and smaller amounts of Bi_2O_3 secondary phase (15cp/150 ^0C) have shown a higher P_r (Table I).

The above results show that the presence of Bi_2O_3 secondary phase deteriorates the ferroelectric properties of SBT capacitors. Although, we could reduce the amount of

this secondary phase by using a bismuth precursor with a high viscosity (15 cp) and a low baking temperature (150 ^{0}C), XRD analysis revealed the Bi_2O_3 secondary phase in small amounts (Fig. 5(b)). Hence we have modified the CSD process to further suppress the formation of Bi_2O_3 secondary phase.

5.4.4 Modified Chemical Solution Deposition Process

Fig. 8 shows the modified chemical solution deposition technique. Bismuth precursor with a viscosity of 15 cp is used to prepare the SBT solution. The modification performed in this CSD process is that after each coating of a very thin layer, the film is baked at 150 ^{0}C followed by annealing at a high temperature of 750 ^{0}C in oxygen atmosphere for 5 minutes. This step is repeated until a final thickness of 0.25 μm is obtained and then, a final annealing is performed at 750 ^{0}C in oxygen atmosphere. The final annealing time is adjusted such that the total thermal duty of this sample is 1.5 hours. For convenience, from here on, we will refer to the SBT thin film prepared using modified CSD process as 'step annealed' sample.

We have observed significantly improved microstructural and electrical properties in step annealed SBT capacitors. Fig. 5.9 shows XRD pattern of step annealed SBT thin film with no observable Bi_2O_3 peak. A comparison between the XRD patterns of Fig. 5.9 and Fig. 5.5 clearly shows that step annealing completely suppresses the formation of the Bi_2O_3 secondary phase. Additionally, micrographs of surface morphology of step annealed SBT thin films revealed uniform grains with the grain size

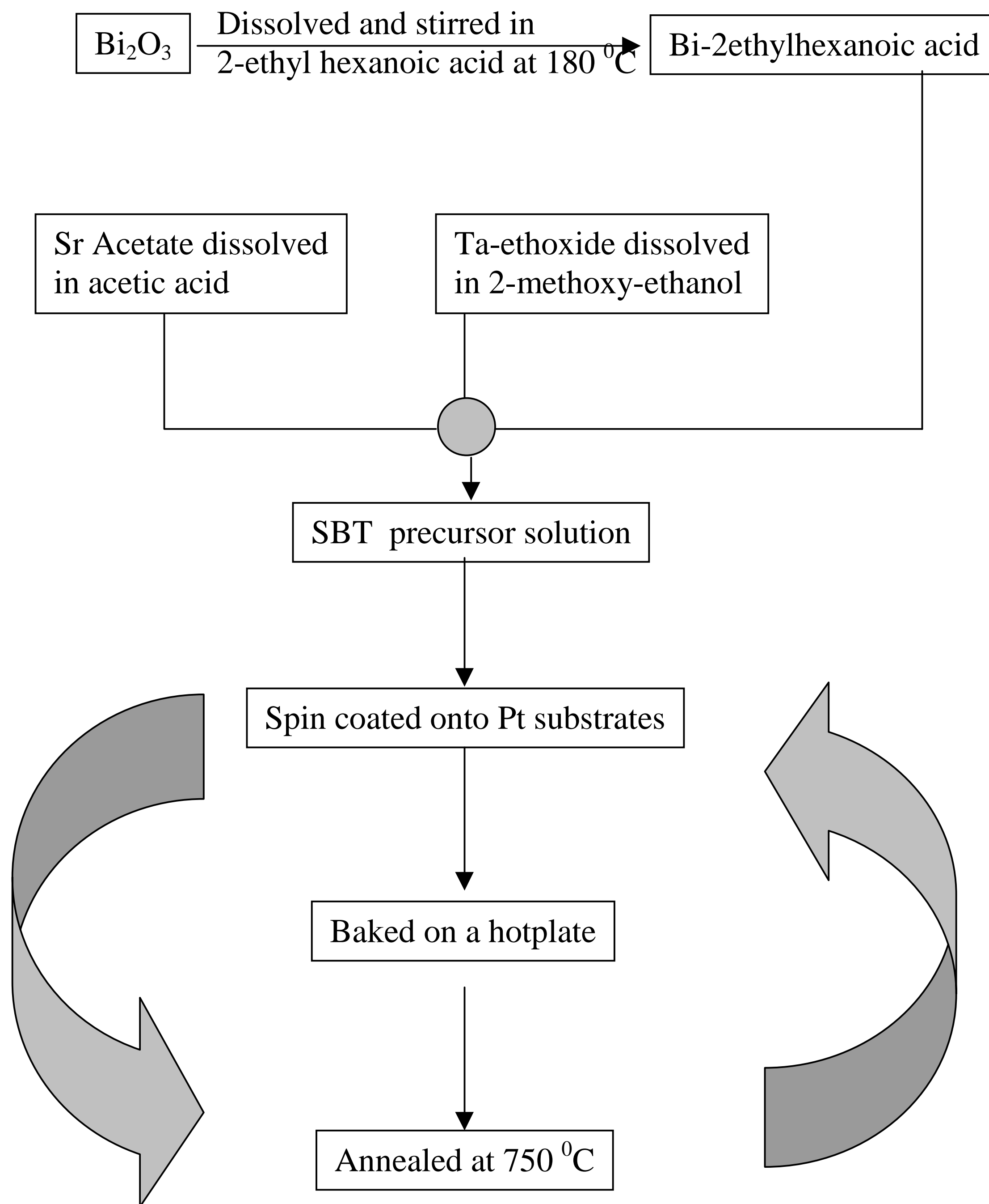

Fig. 5.8. Modified chemical solution deposition method.

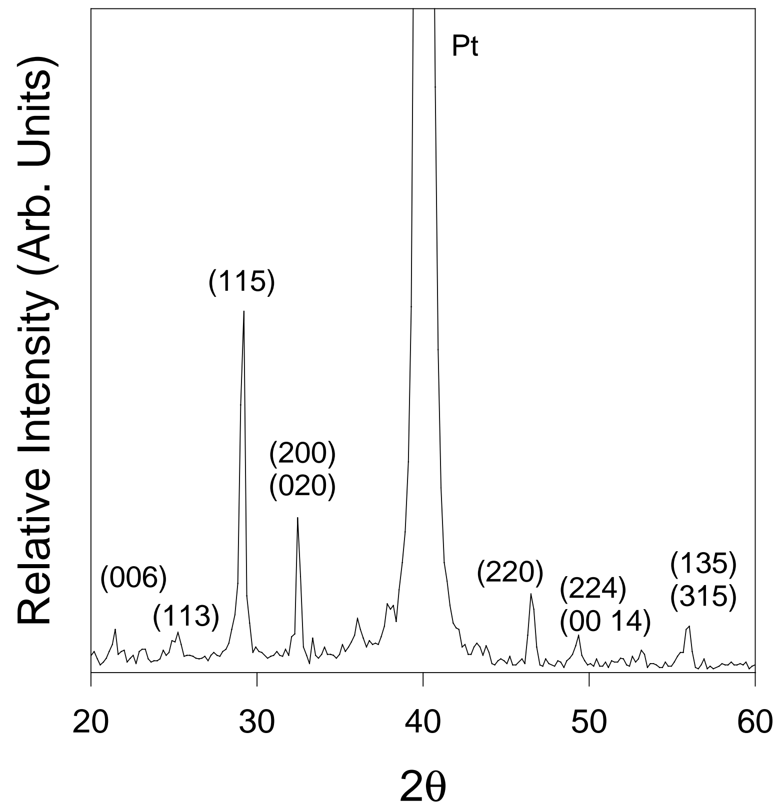

Fig 5.9 XRD pattern of crystallized SBT thin films fabricated using modified CSD process.

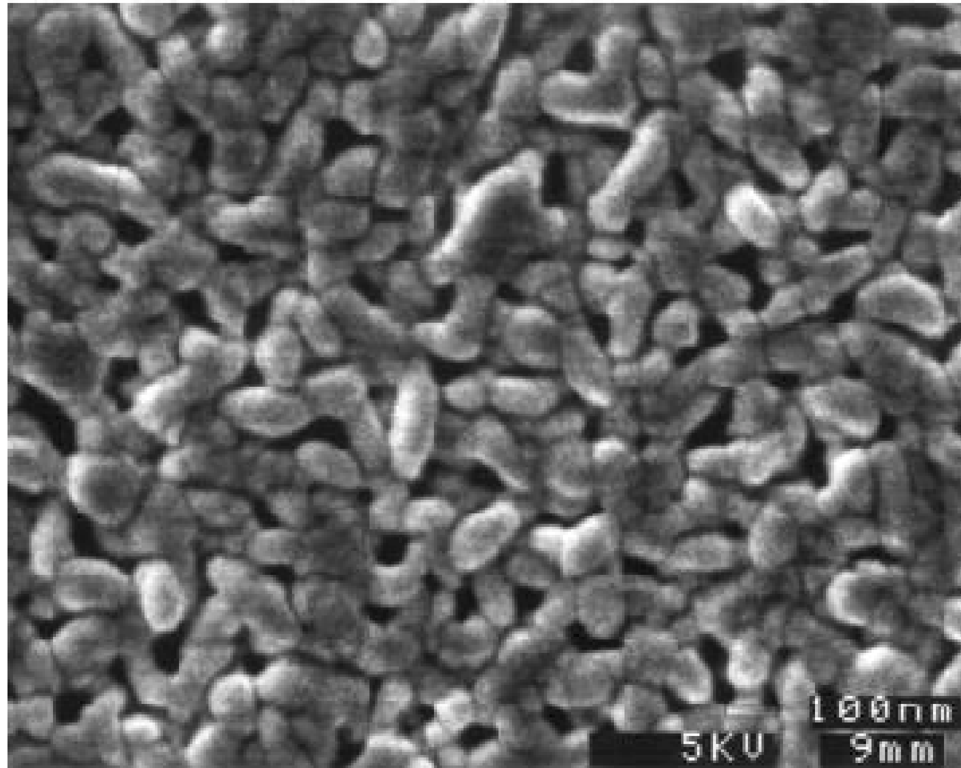

Fig. 5.10 FESEM images of surfaces of crystallized SBT thin film fabricated using modified CSD process

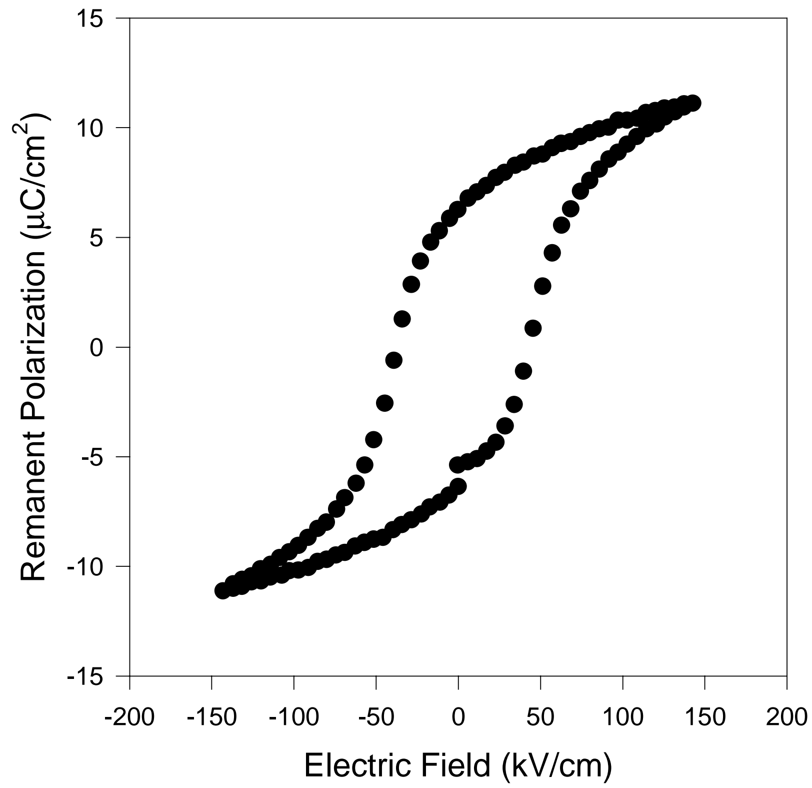

Fig 5.11 Hysteresis loop of SBT thin film capacitor fabricated using modified CSD process.

as large as 165 nm, as shown in Fig. 5.10. There was no bimodular distribution of grains in contrast to the films prepared using conventional CSD process. Consequently, step annealed SBT thin film capacitor exhibited a well saturated hysteresis loop with a high P_r of 7.2 μC/cm^2, as shown in Fig. 11. Although the difference in hysteresis properties exhibited by the step-annealed sample and the 15cp/150 ^{0}C is small, the step-annealed sample exhibited superior ageing characteristics.

5.4.5 Ageing Effects

Ageing of SBT thin films is studied in terms of reduction in P_r with time elapsed after the fabrication of the capacitor. Fig. 5.12 compares the ageing characteristics of SBT thin films processed under different conditions. While P_r of 8 cp/350 ^{0}C sample aged from an original value of 2.1 μC/cm^2 to a value of 1.1 μC/cm^2 in 7 days, P_r of 15 cp/150 ^{0}C sample reduced from a value of 6.3 μC/cm^2 to a value of 5.4 μC/cm^2. Step annealed SBT capacitor exhibited negligible ageing. In the earlier discussions of the current paper, we have shown a strong dependence of processing parameters on the amount of Bi_2O_3 secondary phase in SBT films. Here, a qualitative model is suggested to explain the dependence of ageing characteristics on the amount of Bi_2O_3 secondary phase in SBT capacitors.

SBT thin film capacitor with Bi_2O_3 secondary phase exhibited asymmetric hysteresis loops. Asymmetry in the hysteresis loop can be quantified as □E_c (= E_{c+} - $|E_{c-}|$). Table I shows a strong correlation between the amount of Bi_2O_3 secondary phase and □E_c of SBT capacitors. As the amount of Bi_2O_3 secondary phase increased, the magnitude of □E_c increased. Separation of bismuth in SBT thin films in the form of

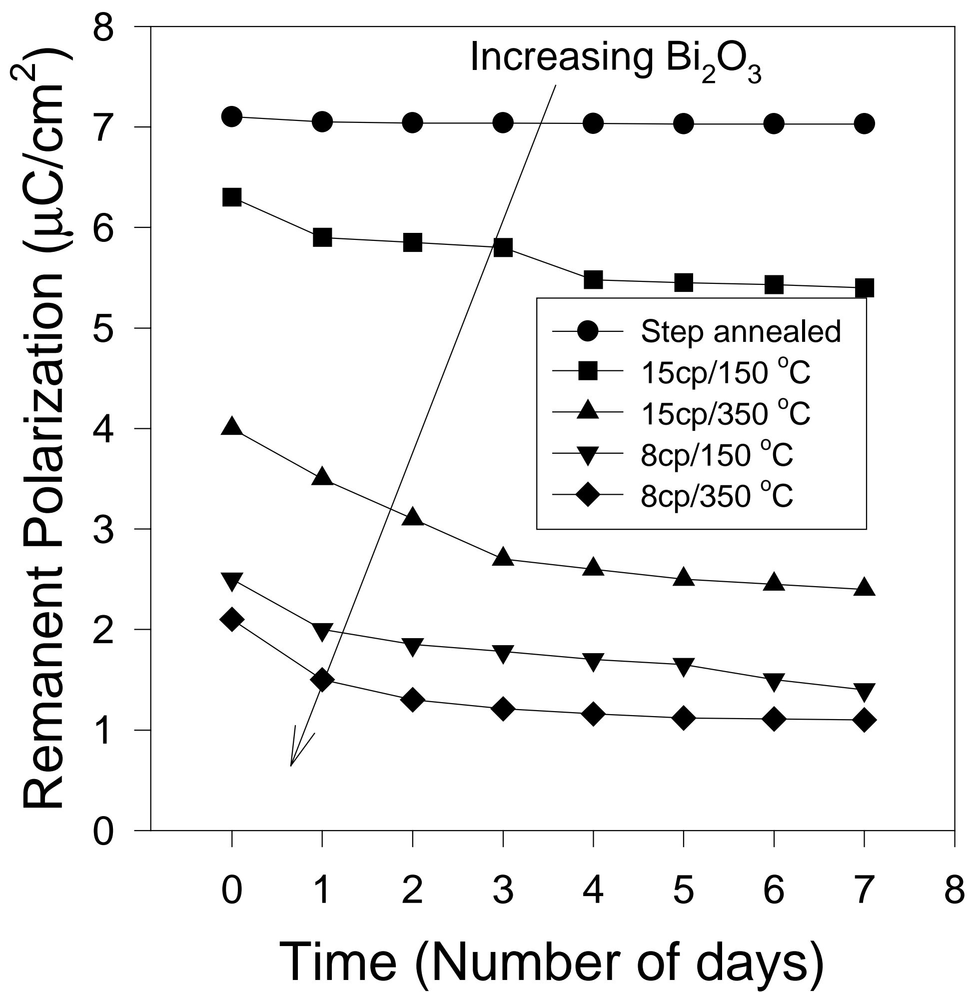

Fig 5.12 Ageing of SBT thin film capacitors fabricated using bismuth precursors with viscosities of 8cp and 15cp; baking temperatures of 150 ^{0}C and 350 ^{0}C; and also ageing of step annealed sample.

Bi_2O_3 secondary phase could yield SBT grains with both bismuth and oxygen vacancies. These vacancies could be a primary source of charged defects which may be inhomogenously distributed. Spatial variation of these charged defects generally result in development of internal fields (E_I). Presence of internal field would tend to bias the coercive field (E_c) in both the directions (E_{c+} and E_{c-}) and their magnitudes depend on the orientation of the internal field with respect to the applied field. For instance, if the internal field and the applied field are oriented in the same sense, then

$$E_{c+} = E_c - E_I \qquad (1)$$

$$E_{c-} = E_c + E_I \qquad (2)$$

$$□E_c = E_{c-} - E_{c+} = 2E_I$$

(3)

Eqn (3) shows that $□E_c$ is directly proportional to the internal field. Since internal field is indicative of non-uniform defect density, $□E_c$ would also represent the non-uniform charged defect density present in the ferroelectric capacitor. Hence, SBT thin films with large amounts of Bi_2O_3 secondary phase, which exhibited high values of $□E_c$, might possess large number of inhomogenous charged defects.

Rate of ageing (or rate of reduction in P_r) in SBT thin film capacitors was found to be dependent on the amount of Bi_2O_3 secondary phase. P_r of step annealed sample, which contained no noticeable Bi_2O_3 secondary phase, aged less than 1% as compared to 48% ageing in 8 cp/350 ^{0}C sample containing large amounts of Bi_2O_3 secondary phase (Fig 5.12). Large amounts of Bi_2O_3 secondary phase in SBT films correspond to the presence of high defect density in the capacitors. Internal field generated due to charged defects could have a significant impact on the domain configuration. Immediately after

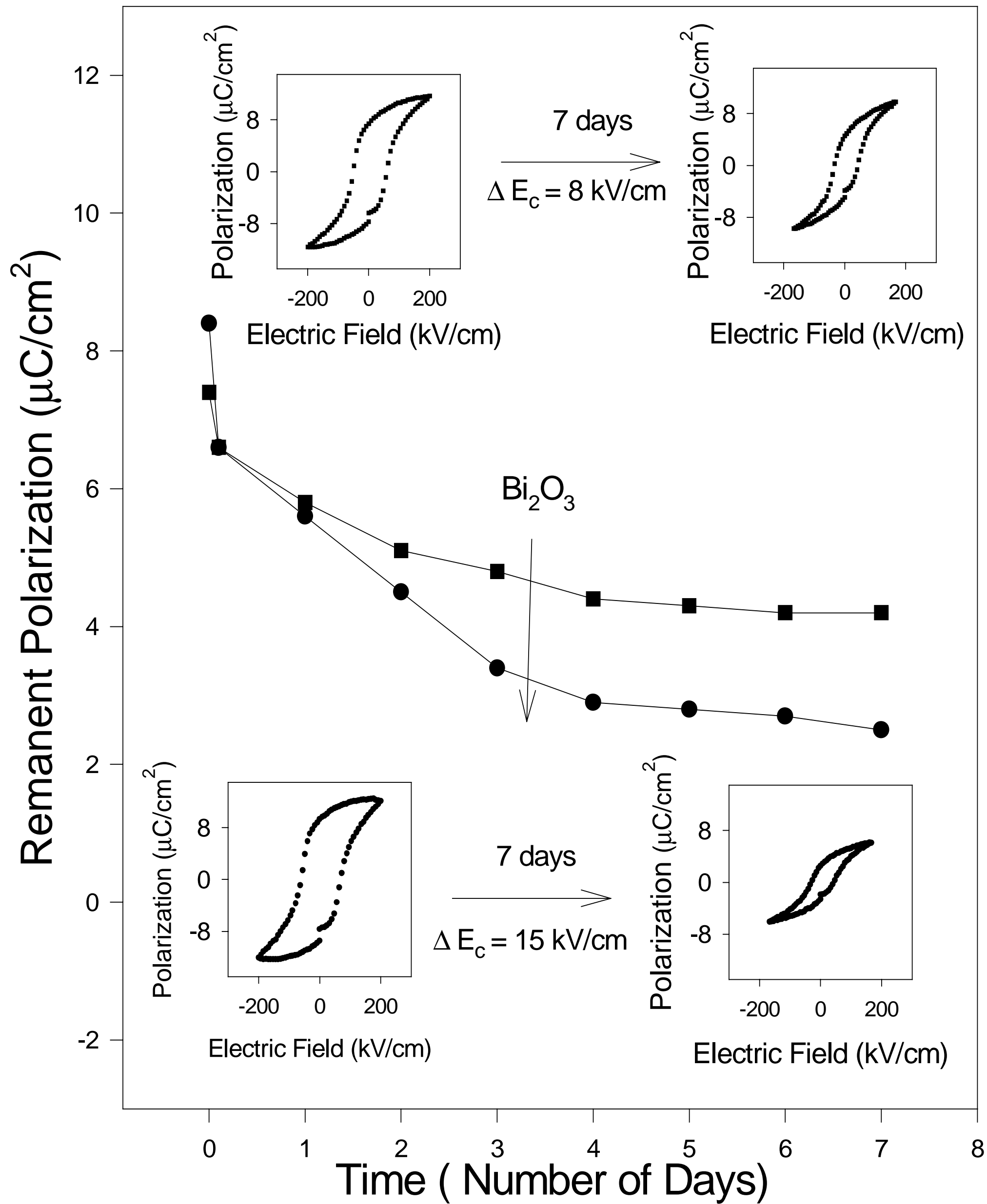

Fig 5.13 Ageing of SBT thin film capacitors shown as a function of amount of Bi_2O_3 secondary phase present in the film. The insets compare the hysteresis loops exhibited on 7th day after the fabrication of SBT capacitor to that of virgin sample.

the fabrication of the SBT capacitor, these defects might not be in their equilibrium configuration. During the migration to the equilibrium positions, some of the charged defects might arrive at the domain boundary and subsequently pin these domains. Pinning could cease the domains from responding to the external field resulting in reduction of P_r. Higher the charged defect density, higher is the number of charged defects that could pin the domains and hence, higher the reduction of P_r. This could explain the significant drop of P_r in SBT capacitors with high amounts of Bi_2O_3 secondary phase (Fig. 5.13), which would possess high defect density. In the case of step annealed SBT sample, we observed no Bi_2O_3 secondary phase (Fig. 5.6). Hysteresis loop exhibited by SBT thin film capacitor fabricated by modified CSD process showed perfect symmetry (Fig. 5.11). Consequently, due to absence of any significant charged defects, we observed negligible reduction of P_r in these samples (Fig. 5.14).

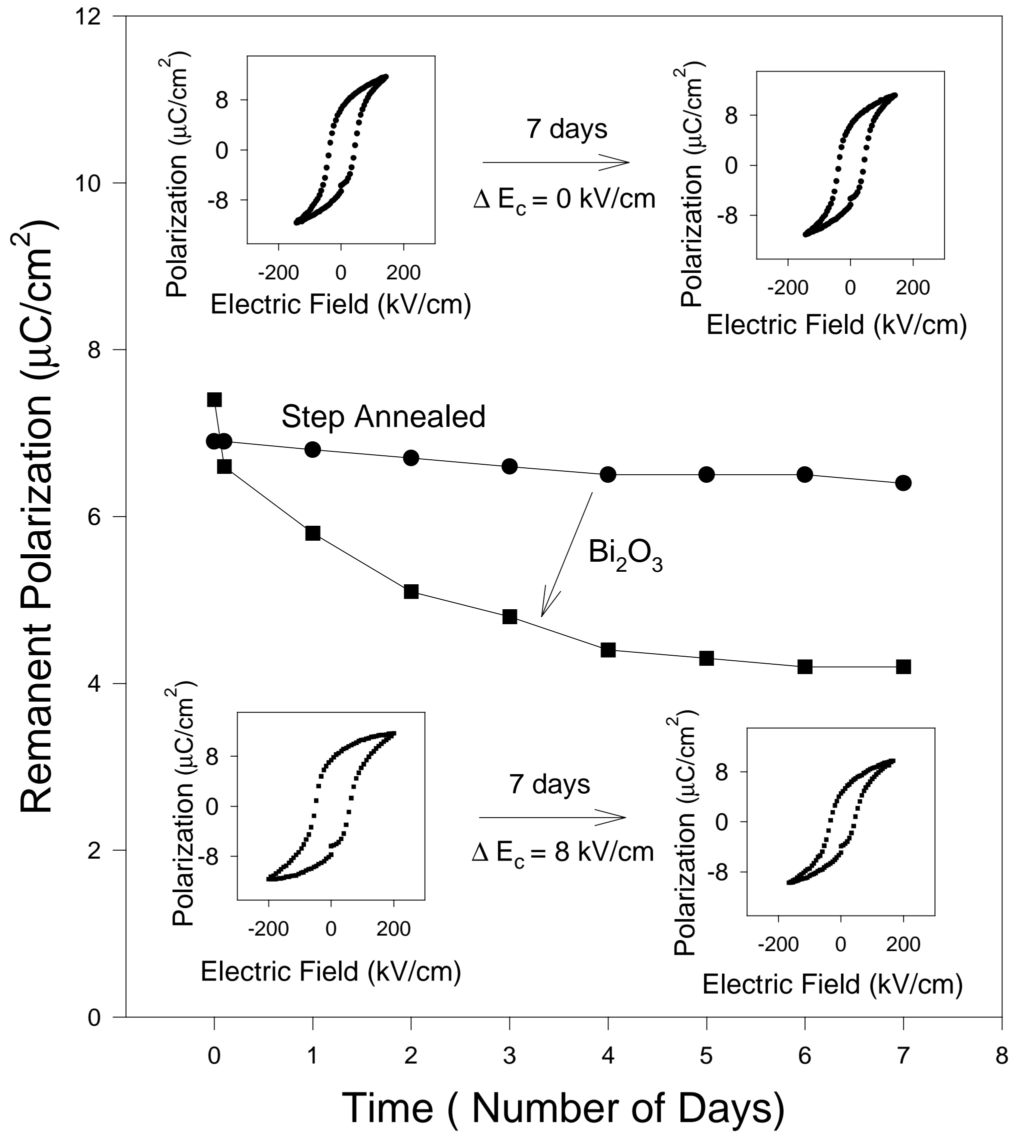

Fig 5.14 Comparison of ageing in step annealed SBT capacitor with that of conventionally prepared sample.

5.5 Conclusions

We identified the viscosity of bismuth precursor and the corresponding baking temperature as two of the processing parameters that could affect the crystallization and ferroelectric properties of SBT thin films in a chemical solution deposition process. Lower viscosity of bismuth precursor and higher baking temperature had resulted in the formation of Bi_2O_3 secondary phase during the baking of as-deposited SBT film. Presence of such secondary phases was found to have a significant effect on the microstructure of SBT thin films. Average size of SBT grains and the remanent polarization of SBT thin film capacitors was found to increase with the decrease in the amount of Bi_2O_3 secondary phase in the crystallized SBT films. Additionally, we also observed increased rate of ageing in the SBT thin films with Bi_2O_3 secondary phase. A modified CSD process was shown to maximally reduce the secondary phase and thereby, yielded SBT thin films with improved microstructure, a high remanent polarization and excellent ageing characteristics. Pinning of the domains by the charged defects could be a reason for the ageing of SBT thin film capacitors with Bi_2O_3 secondary phase.

Acknowledgements

One of the authors (S. Tirumala) would like to thank R. Vedula, S. Kaza, C. Desu, S. O. Ryu and L. Rabouin for their useful discussions on the presented study.

References

1. C. A-paz de Araujo, J. D. Cuchlaro, L. D. McMillan, M. C. Scott and J. F. Scott, Nature **374**, 627 (1995).
2. P. C. Joshi, S. O. Ryu, X. Zhang and S. B. Desu, Appl. Phys. Lett. **710**, 1080 (1997).
3. T. Noguchi, T. Hase and Y. Miyasaka, Jpn. J. Appl. Phys. Pt. 1 **35, 9B** , 4900 (1996).
4. I. Koiwa, K. Tani, J. Mita and T. Iwabuchi, Jpn. J. Appl. Phys. Pt. 1 **37, 1**, 192 (1998).
5. T. Hayashi, T. Hara and H. Takahashi, Jpn. J. Appl. Phys. Pt. 1 **36, 9B** , 5900 (1997).
6. T. Osaka, A. Sakakbara, T. Seki, S. Ono, I. Koiwa and A. Hashimoto, Jpn. J. Appl. Phys. Pt. 1 **37, 2**, 597 (1998).
7. K. kato, Jpn. J. Appl. Phys. Pt. 1 **37, 9B** , 5178 (1996).
8. S. Ohfuji and M. Itsumi, Jpn. J. Appl. Phys. Pt. 1 **37, 5A** , 2559 (1998).
9. K. Miura and M. Tanaka, Jpn. J. Appl. Phys. Pt. 1 **37, 5A** , 2554 (1998).
10. Y. Tori, K. tato, A. Tsuzuki, H. J. hwang and S. K. Dey, J. Mater. Sci. Lett. **17**, 827 (1998).
11. Y. Ito, M. Ushikubo, S. Yokoyama, H. Matsunaga, T. Atsuki, T. Yonozawa and K. Ogi, Jpn. J. Appl. Phys. Pt. 1 **35, 9B** , 4925 (1996).
12. Tze-Chuin Chen, Ph. D. Dissertation, Virginia Tech., (1995).
13. I. Koiwa, Y. Okada, J. Mita, A. Hashimoto and Y. Sawada Jpn. J. Appl. Phys. Pt. 1 **36, 9B** , 5903 (1995).
14. S. B. Desu and D. P. Vijay, Mater. Sci. Engg. **B32**, 75 (1995).